

1. Introduction :

The family of Hg- based superconductors ($\text{HgBa}_2\text{Ca}_{n-1}\text{Cu}_n\text{O}_{2n+2}$) with a maximum T_c of 134 and 164 K, as measured at ambient and high-pressure respectively (for $n=3$) [1] is still attracting much attention among the cuprates, due to the high superconducting transition temperatures and simple tetragonal structures that provide, conceptually, ideal media to study fundamental crystallographic properties. Parallel research in related structures, such as the $\text{Hg}_{1-x}\text{Tl}_x\text{Ba}_2\text{Ca}_2\text{Cu}_3\text{O}_8$ and $\text{Tl}_2\text{Ba}_2\text{CuO}_6$ compounds, provides interesting substrates for studying intrinsic local phenomena as “stripes” [2] and for probing the superconducting wave function symmetry [3]. Further, the synthesis of Hg-based thin films offers possibilities for electronic applications above 110 K. A high critical current density, J_c , of about 10^6 Acm^{-2} at 77 K [4], and the development of a superconducting quantum interference device SQUID operating above 110 K [5] have been reported.

Recently, high-quality $\text{Hg}_{1-x}\text{Tl}_x\text{Ba}_2\text{Ca}_2\text{Cu}_3\text{O}_{8+\delta}$ [2, **Error! Bookmark not defined.**] and $\text{Tl}_2\text{Ba}_2\text{CuO}_{6+\delta}$ thin films have been produced [6]. However, current applications are still hindered due to a lack of reproducibility of high quality thin film growth. *In situ* growth of such films in vacuum conditions is difficult due to the high volatility of the highly toxic Hg and Tl, and due to the high sensitivity of barium ions to humidity and carbon dioxide. Although the crystalline properties of thin films could be expected to be similar to the corresponding bulk superconductors [7], some of the structural and physical characteristics exhibit distinct differences. Such is the case for the c-axis lattice parameter and T_c , as compared to the bulk, which usually exhibit lower values. Since the T_c values in these thin films are still relatively high, the large variation in the c-axis unit cell lengths cannot be solely explained by the different oxygen content, δ . The commonly used techniques, such as scanning electron microscopy and X-ray diffraction, do not provide sufficient information about the atomic structure to elucidate the observed discrepancies, the latter requiring a

detailed structural analysis. In particular, probing the composition depth distribution and the evolution of contaminants upon annealing can help to understand and control the superconducting properties and the stability of these materials.

In this work we have studied the composition, crystallinity, uniformity, purity, and thermal stability of $\text{HgBa}_2\text{CuO}_{(4+\delta)}$, $\text{Hg}_x\text{Tl}_{1-x}\text{Ba}_2\text{Ca}_2\text{Cu}_3\text{O}_{(2n+\delta)}$ and $\text{Tl}_{1.85}\text{Ba}_2\text{CuO}_6/\text{LaAlO}_3$, either in bulk or as epitaxial thin films, by Rutherford backscattering and channeling spectrometry, and He^+ and H^+ *non-Rutherford* resonant scattering.

2. Experimental :

Each type of material was obtained with a specific growth technique at a different laboratory. Pellets of Hg1201 were produced in Grenoble by solid state reaction of $\text{Ba}_2\text{CuO}_{3+\delta}$ and HgO precursors at 900°C under 20 kbar pressure on a belt-type apparatus [8], with a T_c (onset) of 89 K. Two pellets of Hg,Tl-1223 were synthesized in Stockholm from mixtures of purified metal oxides and heated in sealed silica tubes as described in ref. [9]. One of the samples was oxidised one week in an oxygen flow at 450°C . T_c was 128 K and 133 K for the non-oxidised and for the oxidised samples, respectively. A Tl-2201 thin film was prepared in Göteborg by laser ablation onto a LaAlO_3 substrate, as described in ref. [10], with T_c (onset) at 49 K. X-ray powder diffraction analysis showed that each sample was essentially free of homologue phases. In the Hg,Tl-1223 system, a small amount of Ba, Ca, CuO containing oxides was detected (5%).

Helium backscattering spectrometry was used to determine the composition and the thickness of the samples as a function of thermal treatment. Backscattered particles were detected at scattering angles of 172° and 110° . Additionally, ion beam channelling was applied to study the crystallinity of the thin films. Since the scattering cross section of the light constituents (i.e. oxygen and carbon) is extremely small compared to the cross sections of the heavier

atoms (such as Hg and Tl), we relied on non-Rutherford resonant scattering [11] to probe these light elements. First, oxygen was probed using the 3.045 MeV alpha resonance, enhancing the cross section approximately 23 times in case of 172° scattering. In all measurements described below, an incident energy of 3.062 MeV was used, hence probing the oxygen content in the near surface region of the samples. Secondly, non-Rutherford resonant scattering on carbon was performed using a 1.75 MeV proton beam and a scattering angle of nearly 180° (resulting in a 70 fold enhancement of the cross section). Prior to performing the experiments, the energy of the incident beam was carefully calibrated using resonant scattering on a SiO₂ thin film.

In situ vacuum annealing ($< 10^{-7}$ Torr) was used to assure exactly the same experimental conditions for all measurements after each thermal processing step.

3. Results :

3.1 Vacuum annealing of HgBa₂CuO_(4+x) pellets

The composition of these superconductors was determined before and after *in situ* vacuum annealing. A first striking observation is that all samples exhibit a significant metal deficiency – mainly Hg – near the surface. Since none of the heavy elements show an increased surface concentration, excess of light masses (carbon contamination, oxygen,...) must be at the origin. In order to interpret the high-energy part of the backscattering spectra (i.e. corresponding to the metals), information on the oxygen content turned out to be indispensable. Figure 1 shows the backscattering spectrum of the as-grown sample, together with a simulation in which a gradual metal deficiency near the surface was assumed. In this simulation, the Hg concentration gradually varies from 0.67 at the surface, to 1 in the bulk of the sample, over a region of approximately 20.000 Å. The data also indicate a tendency for a slight Cu deficiency. From the analysis, it became clear that excess oxygen largely

compensates the missing metal fraction, its concentration increasing from the bulk value of 4 up to a value of 5 at the surface.

However, the spectra cannot be interpreted as oxygen simply replacing all missing metal atoms, thus suggesting that other light impurities (which remain below the backscattering detection limit) are present as well. Optimal fits, as the one shown in Fig. 1, were typically obtained by introducing a surface carbon concentration of the order of 10 %. In order to get direct evidence for the presence of carbon, resonance measurements were done using a 1.75 MeV proton beam. Within the probing region of the H^+ beam, i.e. the first 500 nm from the surface, a carbon concentration of approximately 12 at. % was deduced (Fig. 2), confirming the idea of a significant carbon contamination conjectured from the He backscattering measurements.

Subsequently, the sample was *in situ* annealed in vacuum at 100°C, 200°C and 300°C respectively. From the backscattering spectra, an enhanced near surface metal depletion is evident, mainly due to an increasing Hg loss with increasing annealing temperature, as well as a minor Cu deficiency. Moreover, from the oxygen part of the spectrum, a clear increase in oxygen content can be deduced. For the sake of clarity, only the spectrum collected after 100°C annealing is shown in Fig. 1. A slightly higher carbon concentration was considered as well in order to optimize the simulation, in agreement with the results obtained with H^+ backscattering.

3.2 Oxidation of $Hg_xTl_{1-x}Ba_2Ca_2Cu_3O_{(2n+2+s)}$ pellets

The composition of the pellets was determined before and after *ex situ* oxidation. These samples as well exhibit a significant deficiency of the metals near the surface. It should be noted that Hg and Tl cannot be resolved in conventional RBS measurements. Hence, the information of these two constituents is combined, and labelled 'HgTl'. Figure 3 shows the

backscattering spectrum of the as-grown sample, together with a simulation in which a gradual metal deficiency near the surface was assumed. In this simulation, the HgTl concentration varies from 0.7 at the surface to its bulk value of 1, in a region extending to approximately 10.000 Å. Similarly, the Ba and Cu concentration increase from 1.9 to 2 and 2.4 to 3 respectively. No information could be obtained from Ca, the signal of which is too weak. Oxygen compensates the metal deficiency to a large extent. However, replacing all missing metal with oxygen atoms leads to a significant overestimate. Similar to the case of $\text{HgBa}_2\text{CuO}_{(4+x)}$ pellets, introducing small amounts of carbon (below the backscattering detection limit) in combination with an increasing oxygen content towards the surface (an increase from 8 in the bulk of the sample, to 10 at the surface), results in the best fit to the spectrum (solid line in Fig. 3).

From a comparison of the spectra before and after oxidation (Fig. 3), it is clear that further – significant ! – metal depletion occurs during the oxygen annealing, compensated by an additional oxygen enrichment of the sample surface region. The HgTl content at the surface further decreases from its value of 0.7 before oxidation, to as low as 0.15 after oxidation (compared to 1 in the bulk material).

3.3 Vacuum annealing of $\text{Tl}_{1.85}\text{Ba}_2\text{CuO}_6/\text{LaAlO}_3$ thin films

The composition, thickness uniformity and crystallinity of the thin films have been studied as a function of *in situ* vacuum annealing. Several general trends can be deduced : (i) the layers have a uniform composition, but exhibit a slight Tl deficiency in the first few hundred Ångström upon annealing, (ii) the layer thickness is laterally non-uniform, and (iii) the crystalline quality is relatively poor and not very sensitive to the annealing conditions. The thickness non-uniformity, which can either indicate surface or interface roughness (or a combination of both), is correlated with the layer composition. Hence, in order to obtain

unique results, consistent analysis of the spectra of both detectors (i.e. with scattering angles of 172° and 110° respectively) is required. As an example, Fig. 4 shows the random and aligned spectra of the as deposited layers, along with the simulated spectrum of a 3150 \AA thick $\text{Tl}_{1.85}\text{Ba}_2\text{Cu}_1\text{O}_6$ film.

Vacuum annealing ($200\text{-}300^\circ\text{C}$) results in a loss of Tl in the first few hundred \AA and a slightly increased roughness. It was found that the non-uniformity of the thickness, estimated to be approximately 2200 \AA , is of the same order as the layer thickness (3150 \AA), and increases slightly with increasing annealing temperature.

4. Conclusion :

All high T_c cuprate superconductors of the Hg-, Tl- and HgTl-family we studied, exhibit significant metal deficiencies – mainly Hg and/or Tl – in the near surface region. An excess of oxygen predominantly compensates this metal loss, although clear evidence of carbon contamination has been observed as well. Both tendencies are enhanced after oxidation or vacuum annealing of the superconductor. We particularly refer to previous work [12], where it was shown that the incorporation of oxygen, generally referred to as “ δ ” in the general formulae, is not limited to the position $[1/2, 1/2, 0]$ (O_s) at the center of the Hg square, but other point-like oxygen-defect complexes must exist, which could not yet be characterised.. The epitaxial layers which were investigated are extremely rough, and of very modest crystalline quality. These deficiencies might become crucial issues – which need to be controlled – when incorporating cuprate superconductors in practical applications, particularly when thin film material is required.

It was also shown that detailed knowledge of the oxygen content, as obtained by non-Rutherford resonant scattering, is a prerequisite for the comprehensive analysis of the sample

composition. Furthermore, combined fitting of the spectra obtained in two different scattering geometries enabled us to deconvolute the roughness and composition of the thin films.

Acknowledgements :

The authors want to acknowledge financial support by the FWO (Fund for Scientific Research, Flanders, Belgium), the Inter University Attraction Pole IUAP P4/10 and the project CERN/P/FIS/40125/2000 from FCT/Lisbon.

Figure Captions

Figure 1 : Helium backscattering spectra of a $\text{HgBa}_2\text{CuO}_{(4+\delta)}$ pellet after growth (o) along with a simulated spectrum (—), and after vacuum annealing at 100°C (----). The scattering angle of the detected particles is 172° .

Figure 2 : Proton backscattering spectra of a $\text{HgBa}_2\text{CuO}_{(4+\delta)}$ pellet after growth (o) along with a simulated spectrum (—). The scattering angle of the detected particles is nearly 180° .

Figure 3 : Helium backscattering spectra of a $\text{Hg}_x\text{Tl}_{1-x}\text{Ba}_2\text{Ca}_2\text{Cu}_3\text{O}_{(2n+2+\delta)}$ pellet after growth (o) and after oxidation (x), along with simulated spectra (—). The scattering angle of the detected particles is 172° .

Figure 4 : Helium backscattering spectra of a $\text{Tl}_{1.85}\text{Ba}_2\text{CuO}_6/\text{LaAlO}_3$ thin film after growth, using random (o) and aligned (+) beam incidence, along with a simulated spectrum (—). The scattering angle of the detected particles is 172° .

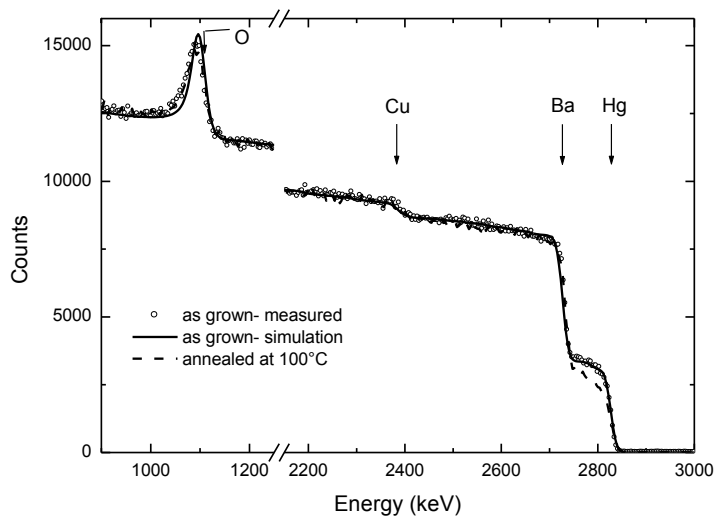


Figure 1 : Helium backscattering spectra of a $\text{HgBa}_2\text{CuO}_{(4+\delta)}$ pellet after growth (o) along with a simulated spectrum (—), and after vacuum annealing at 300°C (----). The scattering angle of the detected particles is 172° .

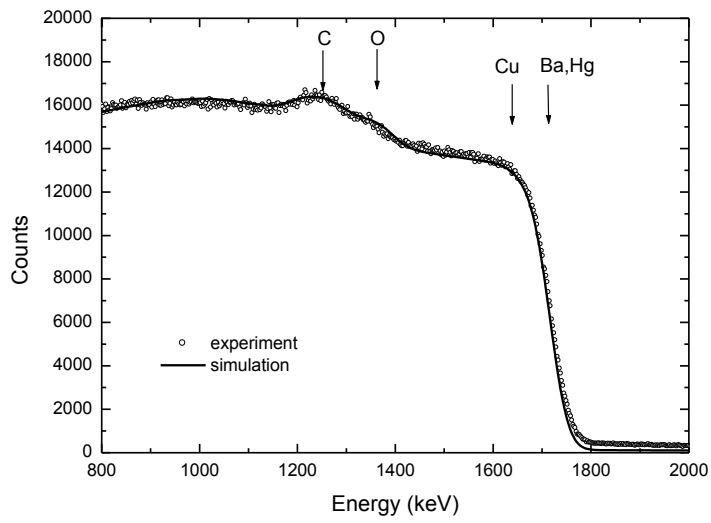


Figure 2 : Proton backscattering spectra of a $\text{HgBa}_2\text{CuO}_{(4+x)}$ pellet after growth (o) along with a simulated spectrum (—). The scattering angle of the detected particles is nearly 180° .

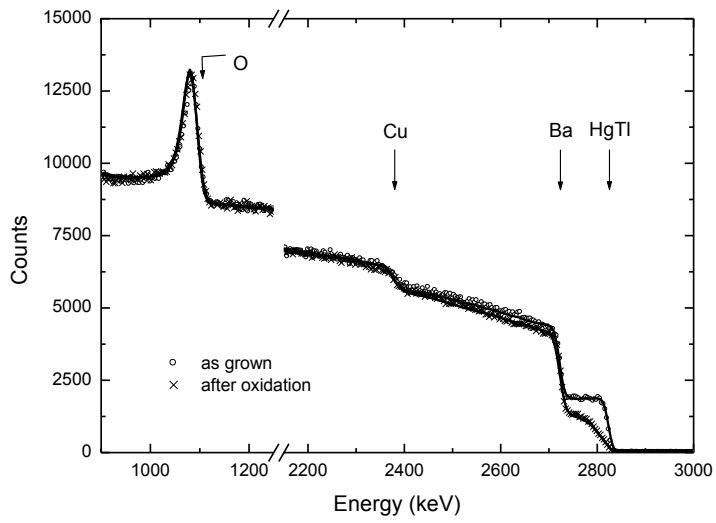


Figure 3 : Helium backscattering spectra of a $\text{Hg}_x\text{Tl}_{1-x}\text{Ba}_2\text{Ca}_2\text{Cu}_3\text{O}_{(2n+2+\delta)}$ pellet after growth (o) and after oxidation (x), along with simulated spectra (—). The scattering angle of the detected particles is 172° .

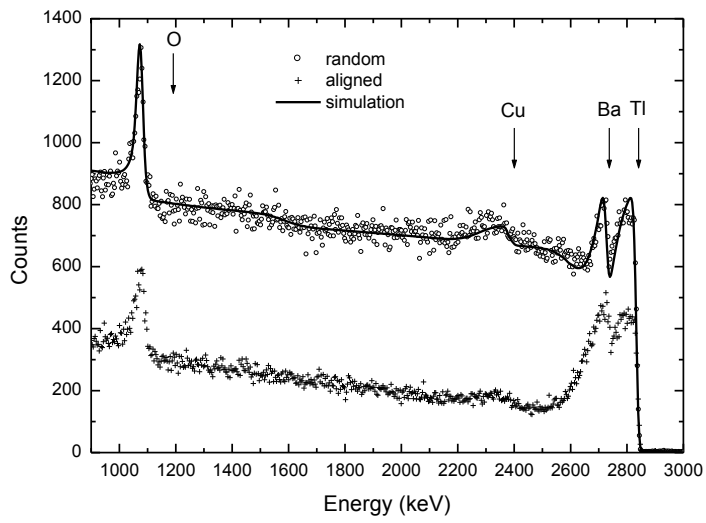


Figure 4 : Helium backscattering spectra of a $Tl_{1.85}Ba_2CuO_6/LaAlO_3$ thin film after growth, using random (o) and aligned (+) beam incidence, along with a simulated spectrum (—). The scattering angle of the detected particles is 172° .

References

- [1] S.N. Putilin, E.V. Antipov, O. Chmaissem, M. Marezio, Nature 362 (1993) 226; A. Schilling, M. Cantoni, J.D. Guo, H.R. Ott, Nature 363 (1993) 56
- [2] S. Titova, I. Bryntse, J. Irvine, B. Mitchell, V. Balakirev, J. Supercond. 11 (1998) 571; S.G. Titova, D.O. Shorikov, V.F. Balakirev, J.T.S. Irvine, I. Bryntse, Physica B 284-288 (2000) 1091
- [3] C. C. Tsuei, J. R. Kirtley, C. C. Chi, L. S. Yu-Jahnes, A. Gupta, T. Shaw, J. Z. Sun, and M. B. Ketchen, Phys. Rev. Lett. 73 (1994) 593; J. R. Kirtley, C. C. Tsuei, J. Z. Sun, C. C. Chi, L. S. Yu-Jahnes, A. Gupta, M. Rupp, and M. B. Ketchen, Nature 373 (1995) 225; C. C. Tsuei, J. R. Kirtley, M. Rupp, J. Z. Sun, A. Gupta, M. B. Ketchen, C. A. Wang, Z. F. Ren, J. H. Wang and M. Buhlan, Science 271 (1996) 329
- [4] L. Krusin-Elbaum, C.C. Tsuei, A. Gupta, Nature 373 (1995) 679
- [5] A. Gupta, J.Z. Sun, C.C. Tsuei, Science 265 (1994) 1075
- [6] H. Q. Chen, L.-G. Johansson, Z. G. Ivanov, App. Phys. Lett. 77 (2000) 1197
- [7] A. Bertinotti, D. Colson, J. Hammann, J-F. Marucco, D. Luzet, A. Pinatel, V. Viallet, Physica C 250 (1995) 213
- [8] S.M. Loureiro, E. V. Antipov, E.T. Alexandre E. Kopnin M.F. Gorius, B. Souletie M. Perroux; R. Argoud, O. Gheorghe, J.L. Tholence and J.J. Capponi, Physica C 235-240 (1994) 905; S.M. Loureiro PhD. Thesis “On the synthesis and structure of Hg-based superconductors”, Lab. Cristallographie, CNRS, Grenoble, (1997) Unpublished
- [9] S. Titova, I. Bryntse, J. Irvine, B. Mitchell, V. Balakirev, J. Supercond. 11 (1998) 571
- [10] H. Q. Chen, L.-G. Johansson, Z. G. Ivanov and D. Erts, Phys. Status Solidi 172 (1999) 165
- [11] J.R. Tesmer and M. Nastasi, *Handbook of modern ion beam materials analysis* (Materials Research Society, Pittsburgh, 1995)
- [12] J. G. Correia, J.P. Araújo, S.M. Loureiro, P. Toulemonde, S. Le Floch, P. Bordet, J.. Capponi, R. Gatt, W. Tröger, B. Ctortecka, T. Butz, H. Haas, J.G. Marques and J.C. Soares, Physical Review B 61 (2000) 11 769